Surface Flux Homogenization and its Impacts on Convection Across CONUS

Tyler Waterman[a] , Paul Dirmeyer[b] , Nathaniel Chaney[a]

[a] *Duke University Civil and Environmental Engineering*

[b] *George Mason University Atmospheric, Oceanic and Earth Sciences Department*

Corresponding author: Tyler Waterman, tyswater@gmail.com

ABSTRACT: In large scale Earth System Models (ESMs) used to study climate processes, surface heterogeneity that is sub-grid to the larger atmospheric grid is often represented by a number of land tiles, effectively providing a higher resolution land surface to a coarser resolution overlying atmosphere. ESMs, however, average the surface fluxes and other surface characteristics before they are communicated to the atmosphere, ignoring the affect that this variability can have on the atmosphere. In this study, we examine the impact of this flux averaging through 257 2-day summer WRF simulations over the Continental United States (CONUS) at 3km resolution, including runs where the surface fluxes and temperature are homogenized at 60 km prior to communication to the overlying atmosphere. Results show large increases (up to 200mm +) in precipitation in moisture limited regions of CONUS, a persistent increase in precipitation bias when compared to observations, and a near universal increase in evaporative fraction. Changes are most significant where moist areas (i.e. water bodies) are averaged with dry areas as the feedback between atmospheric moisture concentrations and the land are weakened when that moisture flux is more spatially distributed through homogenization. Results also show a significant decline in mesoscale flow activity within the atmospheric boundary layer, which in energy limited regions may cause the observed decreases in precipitation due to less frequent convective initiation. Overall, results indicate that flux averaging applied in large scale models can have unintended consequences by neglecting the heterogeneous imprint of the surface on the atmosphere.

SIGNIFICANCE STATEMENT: This work examines what happens when higher resolution information from the land surface is averaged and homogenized before being communicated to the atmosphere in coarse-resolution models such as climate models. Results show that this homogenization can yield significant changes (up to 100% increase) in precipitation in some regions. The most dramatic changes tend to appear when wet areas, including lakes and coastlines, are averaged with the land. Many climate models average ocean and land in atmospheric exchange, which may lead to errors in the water cycle and long term climate prediction. Significant changes to mesoscale atmospheric flows are also observed which may impact convective initiation, however more work is encouraged to assess this aspect of atmospheric impact.

1. Introduction

Weather and climate prediction schemes increasingly seek to represent the complexity of heterogeneous land surfaces and their connection to the atmosphere. How well this heterogeneous land-atmosphere coupling is represented can have significant impacts on accurate representation of local and global water and energy cycles. The complexity of the land surface comes from a variety of state variables and landscape characteristics that directly impact these cycles, including vegetation type, vegetation density, soil texture (Chaney et al. 2019; Xu et al. 2023), soil moisture, groundwater,(Barlage et al. 2021) topography, and surface temperature (Koch et al. 2017; Fisher and Koven 2020). Many of these characteristics vary in space at local (1-100 m) (Vergopolan et al. 2022) and regional scales (1 - 100 km) and in time ranging from minutes to decades. The spatiotemporal variability of these variables has a complex and nonlinear impact on the global system (Santanello et al. 2018; Jung et al. 2011). Modeling work has shown that significant differences occur in land surface state variables with even moderate levels of homogenization approaching local scales (Torres-Rojas et al. 2022; Zhao and Li 2015). Understanding the impact of this heterogeneity on the atmosphere, and how we model it, is critical for accurate model forecasts that tackle complex, multi-scale, modern, challenges in weather and climate.

The land surface affects the atmosphere most directly through the surface fluxes of moisture (latent heat flux) and heat (sensible heat flux). The organization of these fluxes, and other variables, can have significant impacts, which have long been an area of interest in boundary layer meteorology and

24

atmospheric sciences (Bou-Zeid et al. 2020). While observational studies exploring heterogeneous surface-atmosphere do exist, most of the previous work has been through high resolution large-eddy simulations (LES). These studies show that surface heterogeneity, particularly in moisture and surface heating, can cause mesoscale and sub-mesoscale atmospheric response, including secondary circulations (van Heerwaarden et al. 2014; Hadfield et al. 1991; Rochetin et al. 2017; Simon et al. 2021; Zhang et al. 2023), roll structures across the terrain (Weaver 2004), sea and lake breeze effects (Miller et al. 2003; Crosman and Horel 2010; Birch et al. 2015; Hock et al. 2022), breeze circulations over land (Segal and Arritt 1992; Rochetin et al. 2017; Lee et al. 2019; Avissar and Liu 1996), internal equilibrium layers (Bou-Zeid et al. 2020), and an overall increase in the sub-mesoscale and mesoscale kinetic energy (MsKE) and activity of the boundary layer (Simon et al. 2021; Weaver et al. 2002; Skamarock et al. 2014; Zhang et al. 2010). These changes to boundary layer dynamics also cause changes to patterns of convection and precipitation, with studies showing earlier initiation of deep convection (Lee et al. 2019; Hock et al. 2022), increased cloud production (Garcia-Carreras et al. 2011), changes in cloud patterns (Avissar and Liu 1996; Rochetin et al. 2017), as well as increases in precipitation (Guillod et al. 2015; Avissar and Liu 1996; Lee et al. 2019; Birch et al. 2015; Barlage et al. 2021). The literature has also shown that many of these atmospheric responses to surface heterogeneity scale with the magnitude and structure of observed variability (Lee et al. 2019; Han et al. 2019; Hadfield et al. 1991; van Heerwaarden et al. 2014; Rochetin et al. 2017).

Regional and global models for weather and climate vary dramatically in how they represent small (sub-grid) scale heterogeneity in the surface, the atmosphere and in the coupling between the two. Land surface models (LSM) are typically used to provide surface information including fluxes of heat and moisture to coupled atmospheric models in numerical weather prediction schemes (NWP) and Earth System Models (ESMs). LSMs have a long history of development focused on better representing land surface complexity, often through mosaic or tiling schemes. These schemes work by dividing the traditional atmospheric grid into multiple sub-grid tiles near the surface, partitioned according to terrain characteristics, land cover, and plant functional type (Chaney et al. 2021; Bonan et al. 2002; Ducharne et al. 2000). Tiling schemes have shown significant improvements in accurate prediction of surface fluxes as compared to using a singular LSM tile per atmospheric grid cell (Toll et al. 2002; Manrique-Suñén et al. 2013; Zhao and Li 2015), however there is still substantial uncertainty from the coupling of a heterogeneous surface to the overlying atmosphere . Most modern large scale models, such as ESMs used to study climate processes, apply a simple homogenization where an area weighted average is computed from the fluxes on each sub-grid tile (Danabasoglu et al. 2020; Golaz et al. 2022; Held et al. 2019) assuming that the lowest atmospheric model level is a sufficient ”blending height” for flux homogenization. The blending height assumption can introduce errors (De Vrese and Hagemann 2016; Bou-Zeid et al. 2020) even in LSMs run offline from a coupled atmosphere (Manrique-Suñén et al. 2013). In some models, including NOAA-GFDL's Earth system Model Version 4 (ESM4) (Dunne et al. 2020; Held et al. 2019) and the US Department of Energy's Energy Exascale Earth System Model (E3SM) (Golaz et al. 2022), the homogenization not only occurs over the land, but surface fluxes from ocean and other open water tiles are homogenized with land surface tiles to produce one flux to the overlying atmospheric grid. In other models, such as the NCAR Community Earth System Model (CESM) (Danabasoglu et al. 2020), the land and ocean are maintained separately, however sub-grid lakes are still homogenized with the surrounding land. Either form of homogenization effectively eliminates the possibility of impactful, complex land-atmosphere interactions such as heterogeneity driven rolls and circulations, from occurring, thereby causing potential errors in convective initiation, cloud development and precipitation. It is especially concerning when landscapes with high flux gradients, such as coastal regions in ESM4 and E3SM, lakes and mountainous terrain, see significant gradient reduction through homogenization. There have been some attempts to develop schemes that account for some of this observed heterogeneity, including allowing the inter-tile heat and moisture variance at the surface to change atmospheric variances (Huang et al. 2022), the use of multiple sub-grid columns to allow for parameterized circulations (Naumann et al. 2019; Waterman et al. 2024), blended atmospheric tiles in the lower boundary layer to bypass the false blending height idea of homogenization (De Vrese et al. 2016), and multi-plume mass flux additions to boundary layer schemes (Sušelj et al. 2013; Witte et al. 2022). These methods, however, often only account for some heterogeneous land-atmosphere interactions and/or have yet to be broadly applied.

Given the changes heterogeneity can cause to convection and precipitation in LES studies that cover ESM grid cell extents, and the broad use of simple surface heterogeneity homogenization in ESMs, it is important to understand how the scale of surface heterogeneity, or the scale of surface homogenization, impacts the atmosphere at regional, continental and global extents examined in ESMs. This is especially critical as some ESMs move to finer, even convective resolving scales (Satoh et al. 2019). A large number of LES studies have examined how surface homogenization impacts the atmosphere (van Heerwaarden et al. 2014; Hadfield et al. 1991; Rochetin et al. 2017; Simon et al. 2021; Zhang et al. 2023; Lee et al. 2019; Garcia-Carreras et al. 2011). These studies, however, are often limited by idealized terrain, unrealistic periodic boundary conditions, one-way coupling, and/or relatively small spatial and temporal extent compared to those applied in NWP and ESMs. Other studies using coarser resolution models have explored homogenization as well. These studies include offline LSM analysis (Manrique-Suñén et al. 2013; Toll et al. 2002), coupled simulations that vary the resolution of land surface properties or specific physics representation (i.e. groundwater) fed into LSMs (Zhang et al. 2010; Zheng et al. 2021; Knist et al. 2020; Barlage et al. 2021) and studies where atmospheric and land grid model resolutions are scaled together (Iorio et al. 2004; Hohenegger and Schar 2007; Hock et al. 2022). These studies show a variety of impacts of homogenization, including significant changes in domain wide fluxes, precipitation and cloud formation, similar to those identified in local LES studies. There is a crucial limitation of these studies, however, for comparison and applications with ESMs. ESMs with tiling schemes run the LSM at an effectively higher resolution, with higher resolution land surface properties defining the grid, and then average the resulting fluxes to an atmospheric grid rather than running the LSM at the same or coarser resolution than the resolution of atmospheric coupling. ESMs, also, cannot be used to study heterogeneous land-atmosphere coupling as the heterogeneous dynamics are not resolved at the coarse ESM grid scale. To fully understand the impact of the flux averaging and reduced heterogeneity in ESM land-atmosphere coupling, we need a to compare over many cases, for large domains, with averaging scales similar to ESMs, and, critically, with the most significant heterogeneity-induced atmospheric phenomena resolved.

2. Methods

a. Simulation Description

We apply a flux homogenization scheme to two different series of simulations. All cases use the Weather Research and Forecasting model (WRF) run at a 3km resolution. For homogenized simulations, however, the surface fluxes (Latent Heat (LH) and Sensible Heat (H) flux) as well

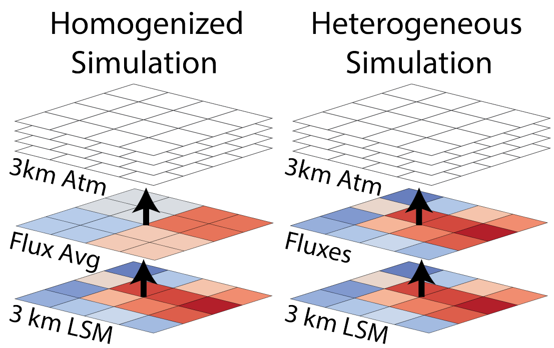

FIG. 1. Illustration showing the homogenization method applied in the WRF simulations. At each time step, the 3km LSM is averaged to some averaging scale before fluxes and surface temperature are communicated to the atmosphere

as the surface temperature are averaged to the homogenization scale before being communicated from the LSM to the atmosphere. That is, fluxes and surface temperature are computed on a 3 km grid, averaged to the homogenization scale, then passed at this coarser scale to the first layer of the 3km atmosphere for every timestep in the simulation as shown in figure 1. It is important to note that no other surface characteristics, including topography, are homogenized. The following two series of simulations are run taking advantage of this homogenization method.

1) Scaling of Homogenization Runs

We use a smaller set of WRF simulations, configuration detailed in section 2b, to provide a basic understanding of how the chosen homogenization scale impacts the simulation. Seven, 48 hour simulations are conducted covering CONUS, northern Mexico and Southern Canada from 2023-07-07 9:00 UTC to 2023-07-09 9:00 UTC at homogenization scales of 3 km (HET), 6 km, 12 km, 15 km, 30 km, 60 km, and 120 km. WRF code modification for homogenization at these scales are included in the code repository (Waterman 2024). These scales of homogenization are selected to cover a wide range of scales, and are somewhat limited by the parallelization of WRF code, which restricts homogenization scales to defined multiples of the grid space allocated to each process by WRF and MPI.

Table 1. WRF simulation grid variables, timestep, and physics options

Grid Extent	1560 x 1040 x 51
Grid Resolution	3 km x 3 km x Stretched
Timestep	Dynamic (~15s)
Microphysics	Thompson Aerosol-Aware (Thompson and Eidhammer 2014)
Radiation	Rapid Radiative Transfer Model (RRTMG) (Iacono et al. 2008)
PBL and Surface Layer	Mellor-Yamada Nakanishi and Niino Level 2.5 (MYNN2) (Nakanishi and Niino 2009; Olson et al. 2019)
Land Surface Model	Rapid Update Cycle LSM (RUC) (Smirnova et al. 2016)

2) Summer Analysis Runs

A much larger series of simulations are used to evaluate changes in the statistics of rainfall and convection more broadly. Two simulations, one that is not homogenized (3 km, HET) and one homogenized at 60 km (HMG), are run for each simulation day. 48 hour HET and HMG simulations are run for every day of June, July and August in the summers of 2021, 2022 and 2023 with most analysis restricted to the second 24 hour period of the simulations. A small number of days in each year were excluded from analysis due to data corruption or model error resulting in a total of 257 HET and HMG simulation days.

b. WRF model configuration

This work uses WRF model version 4.3 (Skamarock et al. 2021) for all simulations, with hourly output retained for analysis. Model is configured similarly to the operational High Resolution Rapid Refresh (HRRR) NWP scheme which is based on WRF (Dowell et al. 2022). A summary of the chosen configuration and physics options are outlined in table 1. Additional details can be found in the namelist files included in the code repository (Waterman 2024). HRRR data is used to provide lateral boundary conditions and initial conditions for each model run.

c. Multi-Source Weighted-Ensemble Precipitation (MSWEP)

To properly evaluate which case, HET or HMG, best reproduces expected patterns of precipitation, we leverage the Multi-Source Weighted-Ensemble Precipitation dataset (MSWEP). MSWEP provides three hourly global precipitation at 0.1 deg resolution (~10km) by merging a large number of gauge based datasets, with satellite data and global reanalysis. The resulting fields are then bias corrected with river discharge observations (Beck et al. 2019). MSWEP was selected for comparison due to its complete coverage of North America and its comparatively high spatial and temporal resolutions.

3. Results

a. Surface Flux Impact of Homogenization

The homogenization scheme has a variety of direct and indirect consequences. Figure 2 shows the instantaneous consequences of the homogenization for one timestep of the scaling simulations. Homogenized fields yield especially significant changes near coastlines and in mountainous regions where sharp gradients occur in the original fields. The fields also shift away from the extreme values, as would be expected with any homogenization.

To provide a more quantitative representation of the loss of spatial information due to a 60 km homogenization, we compute the spatial standard deviation of the 60 km homogenization areas across the 3km domain as shown in figure 3a and 3b. This figure shows the mean of the variability across all three summers, representing the information lost by homogenization. A significant loss of information is shown for both sensible and latent heat flux across much of CONUS, especially in the western Gulf Coast into Texas, Mid-Atlantic Coast, the Great Lakes region, Pacific Northwest, the Central Valley of California and the mountain Southwest including the Sierra Madre Occidental in western Mexico. Notably, latent and sensible heat flux differ in observed heterogeneity between the East and West coast, with the entire West coast having large information loss in H but lower information loss in LH, whereas the East Coast has large information loss in LH and low information loss in H, likely due to the significant difference in ocean temperature between the cool West Coast and warm East Coast.

The coefficient of variation, defined as $CV = \frac{\sigma_X}{\mu_X}$, where σ_X and μ_X are the 60 km standard deviation and mean respectively for flux X, is used to show how the scale of information loss compares with the mean in figure 3c and 3d. Values greater than one generally indicate that the variability loss is more significant than the mean, and values below indicate that it is less significant than the mean. Through this analysis, clearer regions of interest appear. In the dry Southwest, in particular, the loss of LH information is much greater than the observed flux. Most of the Eastern United states, by contrast, has observed information loss significantly below the mean for LH. H,

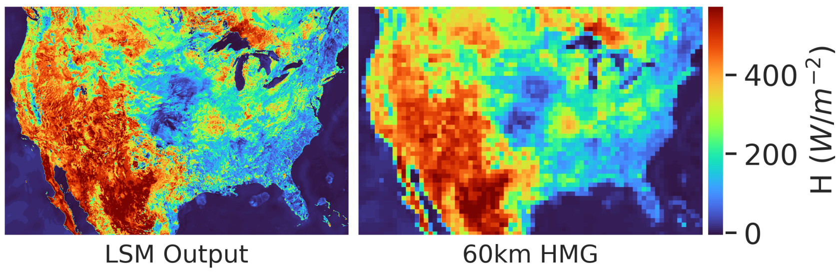

FIG. 2. Comparison of the 3km sensible heat flux (H) fields before (left) and after (right) 60km averaging for 2023-07-08 at 18:00 UTC.

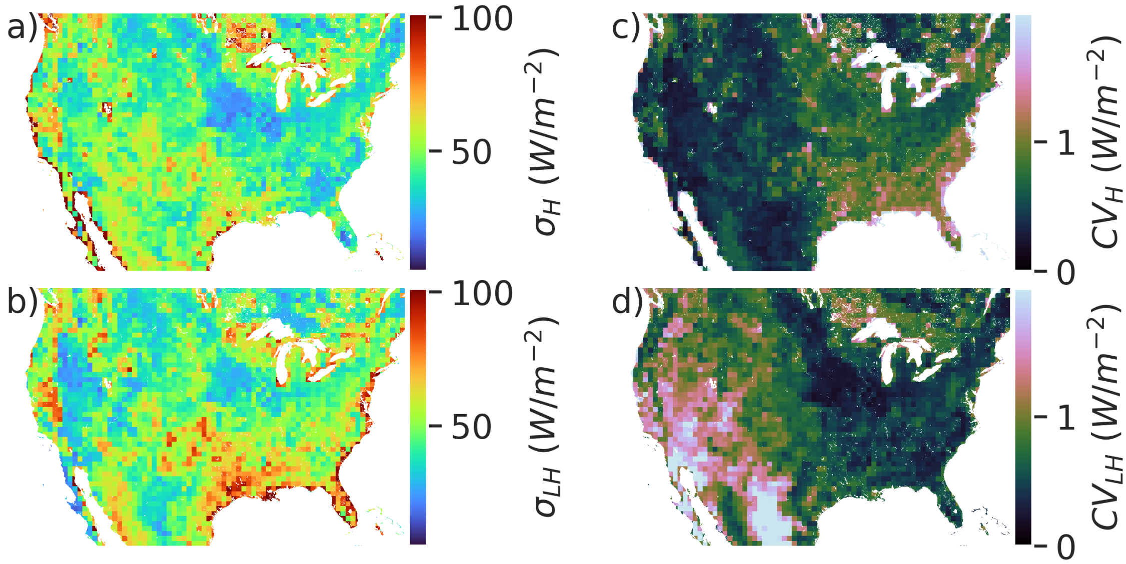

FIG. 3. On the left, spatial standard deviation of the 3km simulation computed at 60km and averaged over JJA 2021,2022 and 2023 for sensible heat flux (a) and latent heat flux (b). On the right, the coefficient of variation for the same fields in (c) and (d).

however, largely shows the opposite with information loss on the order of the mean in the Southeast, and significantly above the mean along the Gulf Coast and West Coast. This is particularly notable due to the relatively high mean sensible heat flux in this region.

There are a few regions where the coefficient of variation is large for both the sensible and latent heat flux, and are therefore likely candidates for observed changes in atmospheric impact. The Great Lakes region as a whole, up to the St. Lawrence River, shows significant information loss in both fields, especially in the northwest and northeast portions of the region. In the Gulf of California, in the Southwest portion of the CONUS domain, close to the coast are numerous points of high CV for sensible heat flux and the region as a whole has large loss of information for latent heat flux. Near the Great Salt Lake there is also high variability loss relative to the mean for both fluxes.

b. Homogenization Across Scales

While the majority of this study focuses on one scale of homogenization, 60 km, it is important to understand how that choice of scale impacts the results of a simulation. The combined effects of changes to the surface fluxes can have a notable impact on simulated precipitation as seen in figure 4. Here, we use Evaporative Fraction (EF), defined as $EF = \frac{LH}{LH+H}$, to represent the relative combination of latent and sensible heat flux. The coarser EF field is apparent in the homogenized case as shown in figure 4b. Figure 4c shows the consequences of this difference through the change in cumulative precipitation between the two cases. Significant differences in the amount and location of precipitation are clear, with the spatial scale of the differences in the central United States on the order of 100 km, and differences in rainfall up to 50 mm. Some regions, for example Western Mexico near the Gulf of California, have significantly greater quantity and spatial coverage of rainfall in the homogenized simulation. Differences in EF in this region are also apparent between the two simulations. This, however, represents only one simulation and as such a more serious discussion and analysis of these phenomenon are reserved for the full summer analysis.

The changes in precipitation that we observe due to the 60 km homogenization do not hold across all scales. We use this difference in precipitation changes to assess the scaling of atmospheric impact and how it relates to the scale of information loss from homogenization. To quantify the changes in precipitation, we use root mean squared difference (RMSD) computed as $RMSD_P = \sqrt{\frac{\Sigma(P_X-P_3)^2}{N}}$ where N is the total number of points, P_X is the total cumulative precipitation at some homogenization scale X and P_3 is the precipitation from the full resolution 3 km model. Figure 5a illustrates how the 6 different homogenization scales change the sensible heat flux over part of the Eastern United States including the southern Great Lakes. The spatial variability of sensible heat flux across CONUS decreases as the homogenization scale increases, signifying a

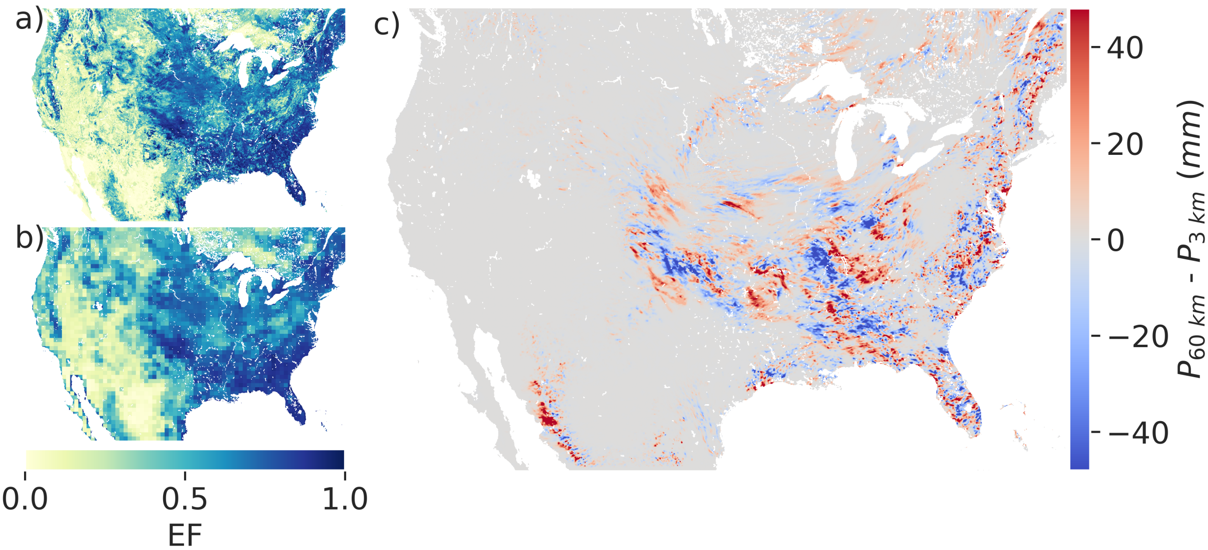

Fig. 4. Comparison between the heterogeneous (3 km; a) and homogenized (60 km; b) noon evaporative fraction as well as the difference in cumulative precipitation between these two cases (c) for the second 24 hour period in a 48 hour simulation that began on 2023-07-07

loss of information, and the deviation of the cumulative precipitation from the heterogeneous case increases. These changes are inverses of each other and are visible in figure 5b, illustrating that loss of spatial variability in the surface flux is closely related to errors in resulting precipitation. Both the loss of spatial variability and the change in RMSD are greatest at smaller scales of homogenization, whereas the differences between larger homogenization scales appear less impactful.

c. Statistics of Precipitation

Precipitation patterns show significant changes over the three summers analyzed in our simulations. We also analyze precipitation patterns observed over three summers from 2021 to 2023. Figure 6 shows the average summer cumulative precipitation for the 3 km HET case (6a) and the 60 km HMG case (6b). Close inspection reveals an overall increase in precipitation in the HMG case, and figures 6c and 6d, which show the difference between the two sets of simulations and the percent difference (spatially smoothed), confirms this fact. The homogenized cases exhibit a mean increase in summer cumulative rainfall over land of almost 25 mm or 17% and median increases of 14 mm or 9.5%. The discrepancies between the spatial means and medians are explained largely

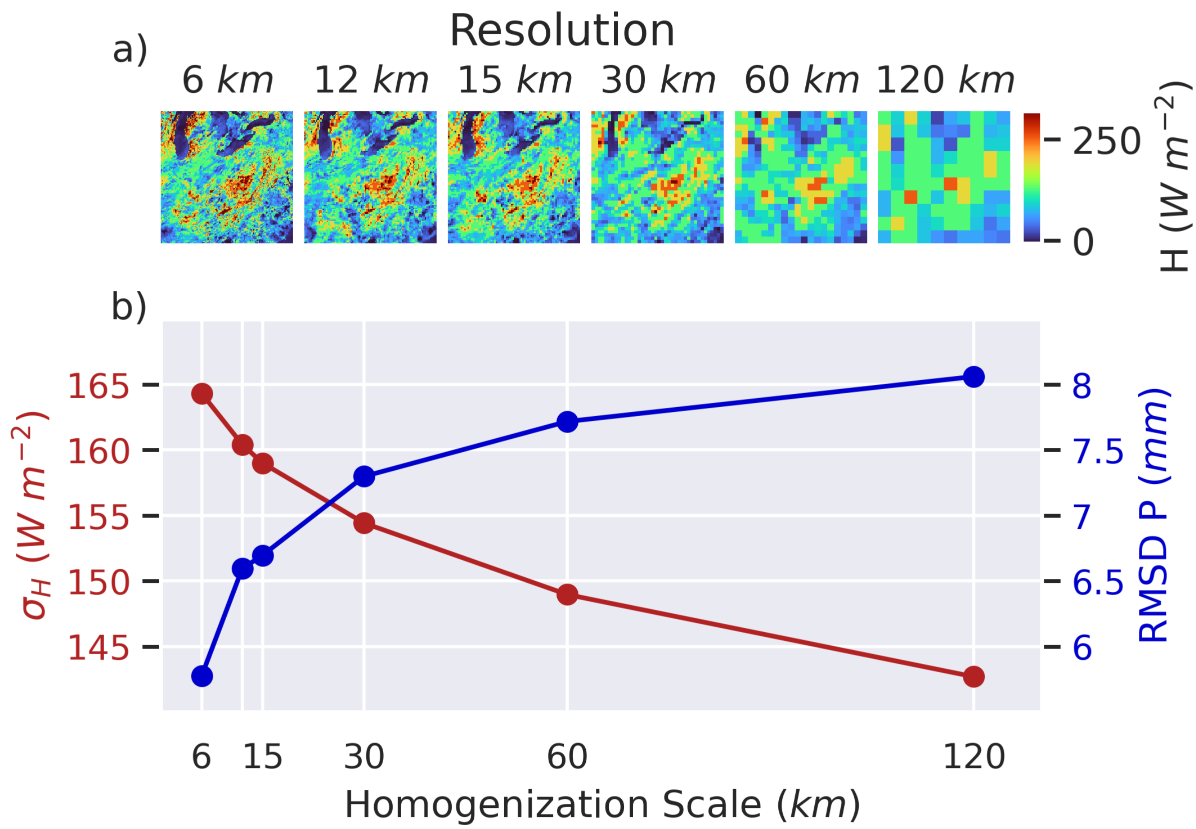

FIG. 5. Images showing the change in sensible heat flux (H) resolution across different homogenization scales in the eastern United States (a), and in (b) the resulting changes in the spatial standard deviation of sensible heat flux (in red; left axis) and the root mean squared difference of precipitation (in blue; right axis) by homogenization scale

explained by the significant outliers, most notably the region of Mexico, California, New Mexico and Arizona near the gulf of California where the rainfall from the North American Monsoon is nearly doubled.

While the changes to the North American Monsoon are the most clear impact of homogenization, there are very significant changes to precipitation patterns in other parts of the domain. Most of the Northeastern portion of the domain, in particular north of the Great Lakes but also including the Mid-Atlantic and New England coastline, also experiences significant increases in precipitation under the 60 km HMG case. With increases on the order of 100 mm and mean precipitation on the order of 300 mm in the 3 km HET case, the change is clearly substantial. Parts of the West

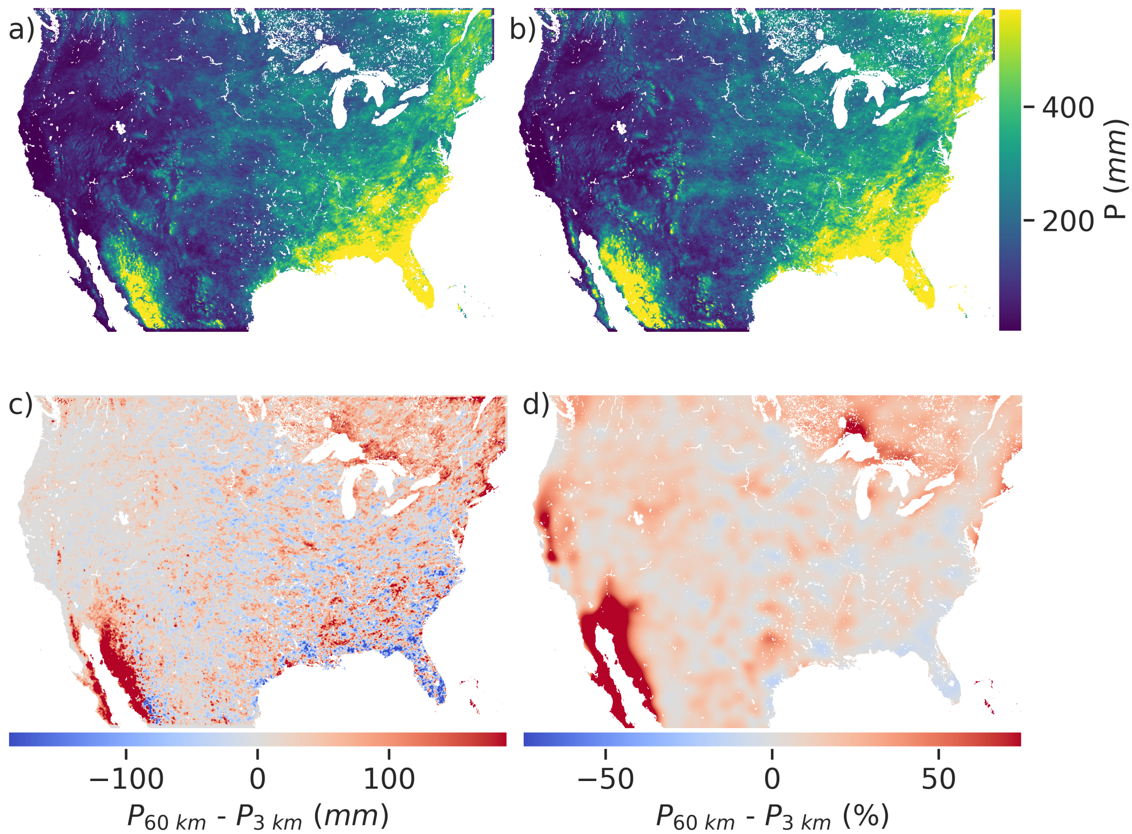

FIG. 6. Precipitation from the second 24 hour period of the 48 hour simulations, accumulated over each of the summers (JJA) and then averaged across the 3 summers for the 3 km (a) and 60 km (b) simulations. The difference in precipitation between the two cases is also shown (c) as well as the difference as a percentage of the mean total summer precipitation for the 3km case (d)

Coast, while experiencing rather low total precipitation, still see significant percentage changes in precipitation.

Patterns across the rest of the domain are weaker and a bit less clear, however. The Mountain West, especially around the Great Salt Lake, has weaker, albeit still significant increases in precipitation due to homogenization. The inland portion of the Eastern United states has significant changes in precipitation, but changes do not have high spatial coherence, implying that changes are either local and small scale, and therefore difficult to interpret with this type of analysis, or that the observed patterns are largely spatial noise. The Southeastern coastal United States, including Florida, is one of the few regions on the map where a large scale persistent decrease in rainfall due

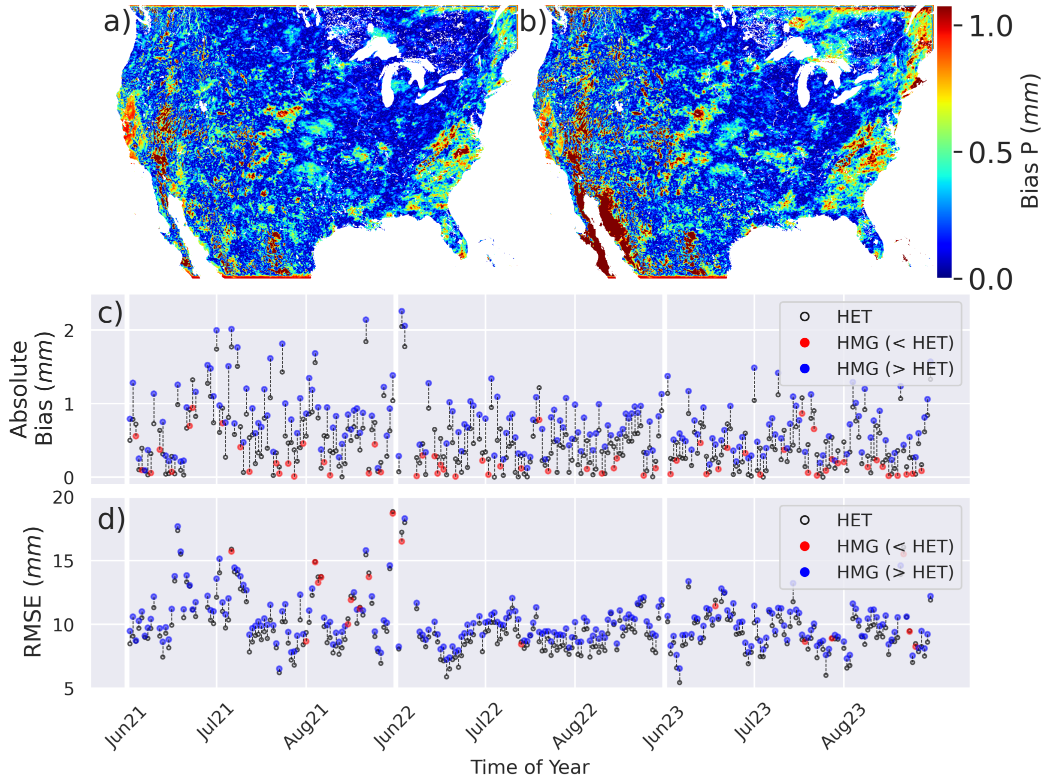

FIG. 7. Comparison of the cumulative precipitation to MSWEP precipitation for the 3km (a) and 60km (b) case. Figure shows the absolute bias (c) and rmse (d) in daily mean simulated precipitation when compared with MSWEP for each simulation day for the Heterogeneous (3 km; HET) case, represented by an unfilled circle, and for the Homogeneous (60 km; HMG) case, represented by filled circles. Circles in red indicate worse performance in the HET case, and circles in blue indicate worse performance for the HMG case

to homogenization may be occurring. It is notable that the regions with significant, or potentially significant changes (Western Mexico, the Great Lakes region, Mid-Atlantic/New England the Great Salt Lake, Central California, Mountain West, and inland Texas) have a significant loss of variability in both latent and sensible heat fluxes due to homogenization (refer back to figures 3a and 3b). There appears, from these two figures, to be a relationship between lost variability and the resulting change in precipitation. Additional exploration of some of these regions and the observed changes will be conducted in the following sections.

The simulated patterns of precipitation can be further compared to observed precipitation using the MSWEP dataset outlined in section 2c. Overall, results show that while both the HET and

HMG case have significant errors compared with MSWEP, the errors are increased with the homogenization in the HMG case. Figure 7a and 7b show the biases of the heterogeneous and homogeneous case respectively. The bias is overall larger in the homogeneous case. Notably, the heterogeneous case appears to make fairly unbiased predictions of the North American Monsoon in Mexico and the Southwestern United States unlike the homogeneous case. Homogenization also appears to increase biases in New England and the Great Lakes region. Examining each of the 257 simulation days individually confirms the persistence of the observed increases in error. Figure 7c shows the absolute bias of the HET case (black open dots) and the HMG case (colored dots). When looking at the observed RMSE, the pattern is even more consistent with the HMG case almost always having more error than the HET case. Only 17 out of the 257 days show that homogenization reduces the error in figure 7d.

d. Changes in Atmospheric Moisture

To further understand the observed changes in precipitation, as well as other changes to the earth system, the difference between the 3 km HET to 60 km HMG case is explored for additional environmental variables. Perhaps the most notable, and spatially universal, change that occurs as a result of the homogenization is that the land becomes broadly wetter, at least in its coupling to the atmosphere. Figure 8c shows that daily mean EF increases across virtually the entire domain due to homogenization, with the most significant increases on the order of 10% close to bodies of water, both small lakes and coastlines, and the largest increases again along the Gulf of California. This increase is largely due to an increase in latent heating, and a very slight decrease in sensible heating. A possible explanation for this is that homogenization of comparatively drier areas with wet areas and bodies of water allows for water to be removed more easily from the wetter areas. The moisture being removed from the wet areas in the HET case only directly impact the overlying atmosphere, which decreases the vertical moisture gradient and dampens the latent heating. When homogenized, the moisture is spread across a larger and dryer domain, instantaneously moves to dry land, and no longer acts significantly to suppress future latent heating. It is worth noting that the locations with the largest changes in EF were also some of the regions with the lowest EF in figures 8a and 8b, and therefore were likely in domains where evaporation is water limited rather than energy limited regime.

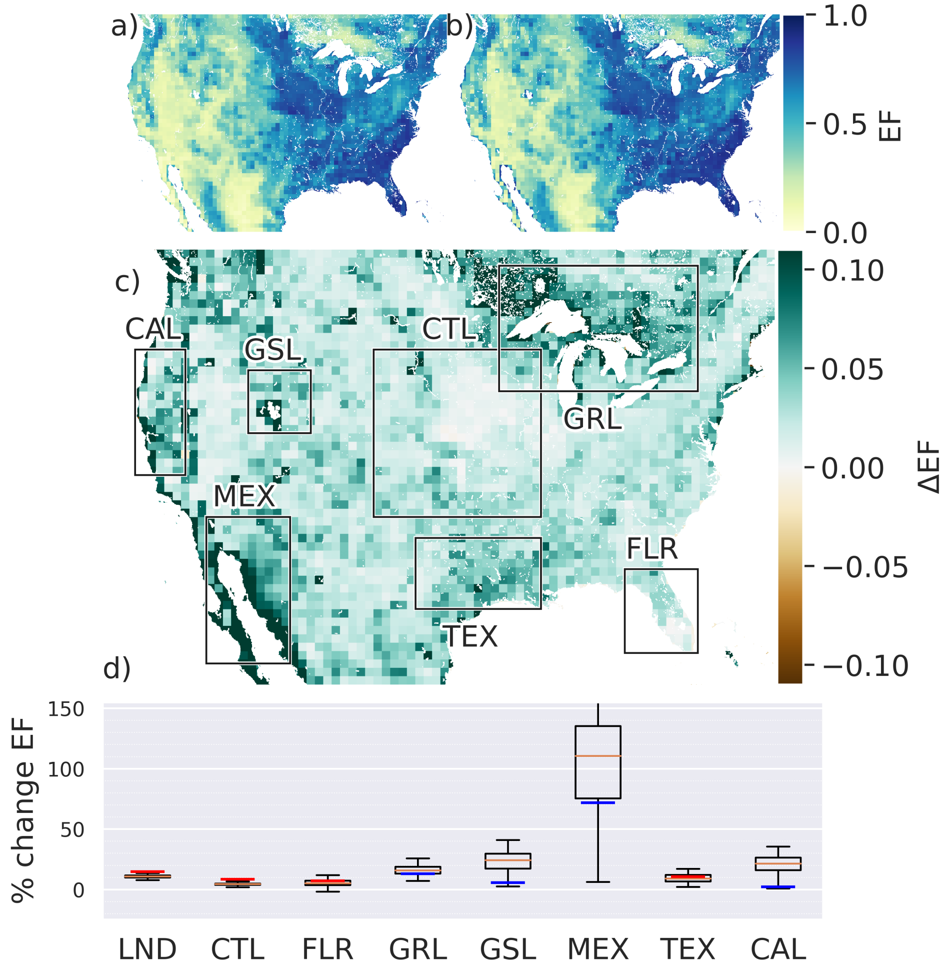

FIG. 8. Daily mean Evaporative fraction EF over the 3 summers at 60km resolution for the 3 km HET case (a) and the 60 km HMG case (b). The difference between them is shown in (c), which also shows the bounding boxes for 7 domains of interest in this study. A boxplot for each domain, including LND representing all land, shows the distribution of the percent change in domain mean EF between the HET and HMG case over the 257 study periods in figure (d). Larger values indicate an increase due to homogenization. Colored bars (blue and red) indicate the median over the 257 study periods, filtered to only include the timestep preceding a rainfall event in the homogenized case. Blue bars indicate a lower median than the full analysis (orange bar), or that before rainfall the difference between HET and HMG was smaller, and red bars indicate a higher median than over the full analysis, or that before rainfall the difference between HET and HMG tended to be larger.

To better examine changes in EF, as well as changes in other phenomena, we divide the domain into 7 regions, in addition to the entire landmass (LND), as seen in figure 8c. The boxplot in figure 8d shows the distribution of the percent change with homogenization in daily, domain-wide mean EF throughout the three summers for the domains defined in 8c. This confirms many of the observations made previously, and shows that the observed trends hold throughout time. Notably, the drier GSL, CAL and MEX domains also show greater variability throughout the season in simulated changes to EF due to homgenization. The figure also helps answer the question of whether the increase in EF is primarily a result of the increased precipitation or a cause of increased precipitation. The colored lines in figure 8d show the median of the change with homogenization in domain-wide mean EF throughout the three summers, but selecting only for times in the simulation immediately preceding precipitation events. That is, they show median change in EF before either the HET or HMG case simulate precipitation. It is clear, looking at the whole domain in LND, that the overall increase in EF occurs before any precipitation. For some domains, notably GSL and CAL, the increase is marginal immediately preceding precipitation events although it is important to note that the sample size of ”pre-rain” timesteps in these domains is poor due to low summer rainfall.

Other atmospheric characteristics are useful to further understand water cycle impacts of homogenization. Homogenization causes an overall increase in precipitable water (PW) in the atmosphere, especially over the west coast and gulf of California, with smaller increases in the GRL region and GSL region (figure 9a. Notably, the increase in PW over the West Coast does not translate to significant increases in precipitation (figure 6c) likely due to the low overall atmospheric moisture availability in this region. All regions with significant PW increases overlap with regions of significant EF increases seen in figure 8, and is likely a direct consequence. Notably, before rainfall events this abundance of PW is not necessarily observed, with decreased PW in the HMG case before rainfall events across all domains. The increase in EF also translates to similar changes in 2 meter relative humidity (RH_{2m}), and the increase is relatively consistent except for a decrease in the pre-rainfall events in the dry low-rain GSL and CAL domains and a decrease in RH_{2m} observed for all situations in Florida, which also saw the smallest increase in PW in the HMG case when compared to the HET case. Low level (300-2000 m) Mid level (2000-6000m) and High Level (6000m +) clouds show a large degree of temporal variability in the boxplots and also the most significant changes as a percent change in mean cloud coverage. Low level cloud cover increases across the entire domain, with the exception of southern Florida, with the greatest increases in

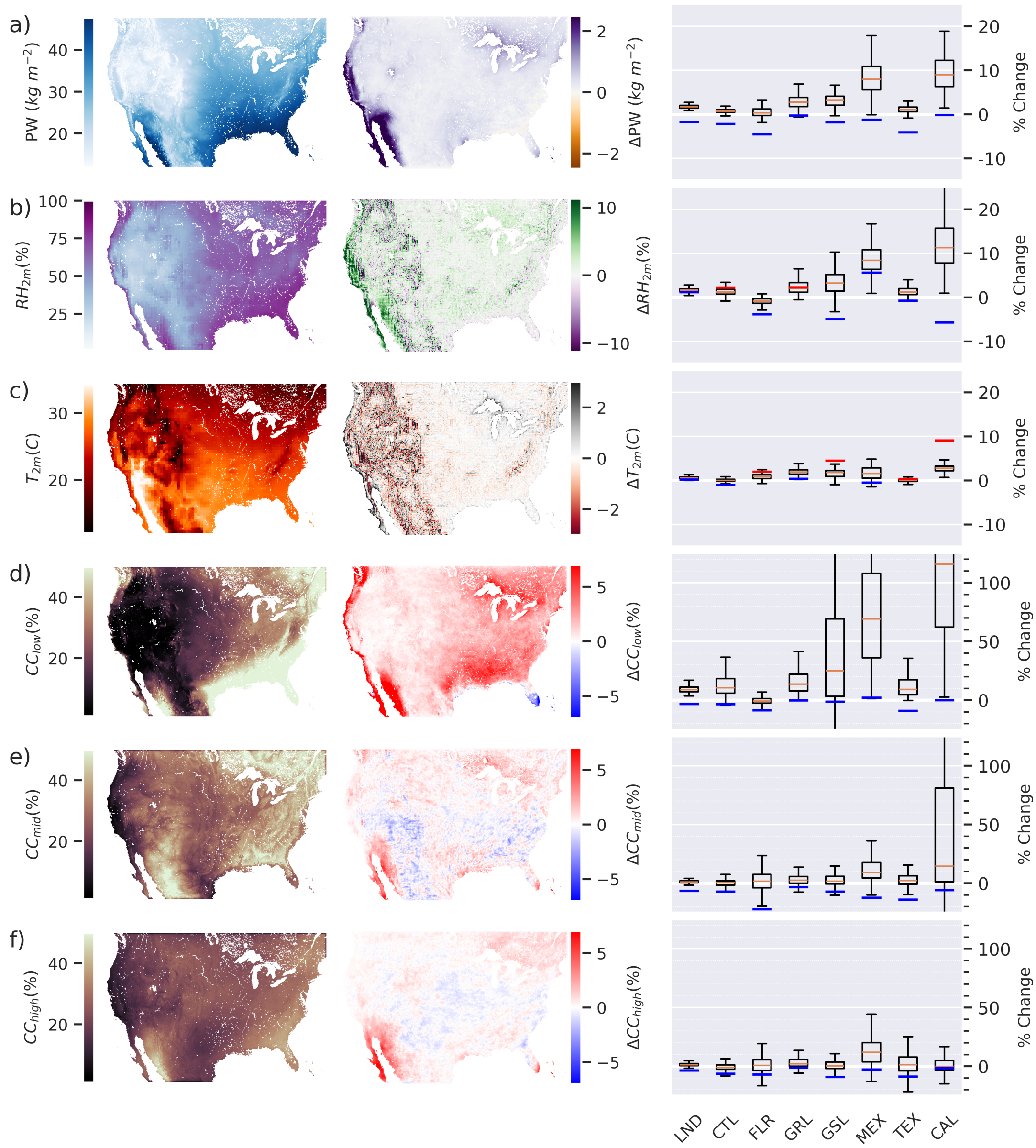

FIG. 9. From left to right in each subfigure, shows the daily mean of a variable over the 3 summers at 60km resolution for the 60 km HMG case (left). The difference between the two cases (60 km HMG - 3 km HET) is shown to the right. A boxplot for each domain defined in figure 8c analogous to figure 8d. Information is shown in each subfigure for precipitable water (PW) (a), 2 meter relative humidity (RH_{2m}), (b), 2 meter relative humidity (T_{2m}), (c), low cloud cover between 300m and 2000m (CC_{low}), (d), mid level cloud cover between 2000m and 6000m (CC_{mid}), (e), and high level cloud cover above 6000m (CC_{high}), (f)

cloud cover over the West Coast and great lakes region. Increases are also present in the South, although this is less significant as a percent change as summer cloud cover is generally high there. Notably much of this increase appears to be during or after rainfall events, as is clear from the right portion of figure 9d. Change in Mid and High level clouds is less spatially consistent, although the MEX region does experience clear increases. In the pre-rain case, the HMG case sees significant decreases in mid and high level cloud cover across all domains. Overall, changes in PW, low level cloud cover, and RH_{2m} appear fairly consistent with simulated EF in figure 8.

e. Mesoscale Kinetic Energy

At first examination, the results of an increase in precipitation and cloud cover appear to defy previous LES studies that show decreases due to the effect of homogenization on mesoscale and sub-mesoscale motion. The indirect changes of flux averaging to mean surface fluxes and EF are provided as an explanation. This, however, begs the question of what happened to heterogeneity driven atmospheric flows. To understand this problem, we use integrated mesoscale kinetic energy (MsKE) applied over 60 km boxes in the domain, which we define as

$$MsKE = \int_0^{z_{top}} \frac{1}{2}(\overline{u'u'} + \overline{v'v'} + \overline{w'w'})\rho dz \tag{1}$$

where ρ is the air density, z_top is the top of the simulated atmosphere, the overline represents spatial averaging over the 60km box, and u',v',w' represent the spatial mean removed velocities in the west-east, north-south and vertical directions respectively. The MsKE can also be viewed as a dispersive kinetic energy analogous to the dispersive momentum fluxes (and kinetic energy) used in previous boundary layer literature (Akinlabi et al. 2022). Although the spatial averaging of this procedure is a bit different than temporal averaging that would be appropriate in boundary layer contexts. This metric should capture mesoscale motions of a scale less than 60km; it will additionally capture mesoscale motion due to storms, however it should be less impacted by larger scale fronts and synoptic scale phenomena. Since most heterogeneity-driven flows are primarily active within the boundary layer, especially near the surface, we additionally define an $MsKE_{low}$, which adjusts the limits of integration to only cover the first 5 pressure levels in the WRF simulation (up to approximately 400 m). This lower level $MsKE_{low}$ will likely be less dominated by larger scale storm cells.

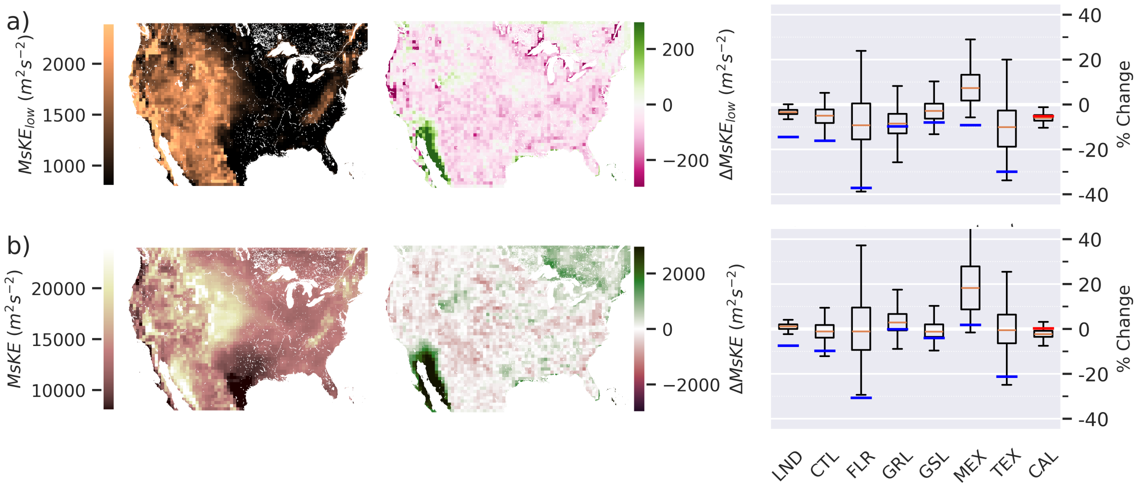

FIG. 10. Subfigure information as in figure 9 for low level vertically integrated mesoscale kinetic energy, approximately 400m and below, ($MsKE_{low}$), (a), and for for total vertically integrated mesoscale kinetic energy ($MsKE$), (b)

MsKE, particularly $MsKE_{low}$, largely conforms with our expectation. Homogenization causes a decrease in $MsKE_{low}$ on the order of 10% across almost the entire domain in figure 10a. Notable exceptions to the trend is part of the GRL Great Lakes region and the Gulf of California (MEX), although the significant increases in rainfall and convective storms in these regions are the likely drivers of these differences. When looking at total magnitude of change, the central and northern west coast and the coastlines of the Great Lakes experience the greatest decrease in mesoscale activity in the ABL due in the HMG case compared to HET, which is likely a signature of the reduction of sea and lake breezes respectively. Interestingly, these same coastlines also appear in the signature of changes in 2 meter temperature (T_{2m}) in figure 9c, where they show significant increases in temperature (2-3 $^{\circ}C$) due to homogenization. This change is likely caused by a combination of reduced sea and lake breezes, clear from the decrease in $MsKE_{low}$, as well as an increase in heating over the bodies of water caused by homogenization. The temperature increase over ocean is not a focus of this study, but likely occurs for reasons analogous to the moisture increase over land; the heat from the land "instantly" transfers to over the ocean without dampening the heat flux over land sufficiently. Although, given that the increased temperature over land would also dampen the heat flux over land, it is unlikely the primary reason for the temperature increases and the changes to cooling sea/lake breezes are likely the primary driver.

The same ”cooling” effect, while present on the coastlines along the Gulf of Mexico and the East Coast, is significantly weaker, likely as these waters are known to be warmer due to the Gulf Stream ocean current coming from the south. These regions, however, still experience changes to the breeze signature of $MsKE_{low}$. TEX and FLR see highly variable changes to $MsKE_{low}$ due to homogenization through time, with a wide distribution of observed changes and median reductions around 10%. Notably, however, when we select only for pre-rain events, homogenization yields a 30 - 40% median decrease in $MsKE_{low}$ and likely sea breezes. In Florida especially, sea breezes are known to cause the initiation of shallow and deep convection (Miller et al. 2003; Crosman and Horel 2010; Hock et al. 2022). Dampened sea breezes are a likely explanation for the decreases in precipitation (and low level cloud cover) in Florida under the HMG case that otherwise defy the continental trends of increased precipitation and cloud cover (see figures 6c, 6d and 9d). More broadly, pre-rain $MsKE$ and $MsKE_{low}$ is either unchanged or significantly reduced due to homogenization in all domains, lending further support to the hypothesized suppression of mesoscale motion from flux homogenization. In non-coastal regions, the homogenization also likely reduces the activity of the most powerful plume updraft structures, as the tail of the sensible heat flux distribution is removed. Overall changes in the fluxes could also cause some of the observed changes, although are unlikely to explain all the phenomena.

4. Discussion

a. Major Effects of Flux Averaging: Interplay between EF and MsKE

The two most direct, and universal, impacts of flux averaging across the three summers of analysis appear to be increases in evaporative fraction EF over CONUS, and a decrease in mesoscale kinetic energy in the lower boundary layer ($MsKE_{low}$) with only highly active storm zones defying the trend. We use $MsKE_{low}$ as a proxy the types of mesoscale motions that heterogeneity is known to enhance, including secondary circulations, plumes, land-lake, land-sea, and land-land breezes. Examining only the $MsKE_{low}$ or only the EF changes between the 60 km HMG and 3 km HET flux averaging cases is insufficient to explain the observed trends in clouds and precipitation; decreases in heterogeneity driven flows are expected to be correlated with decreases in cloud production and precipitation, however much of CONUS shows an average increase. Similarly, increased moisture in the atmosphere due to increased EF is widely observed across CONUS, but this increased moisture fails to translate to increased precipitation, high, or mid level clouds over much of CONUS and decreased precipitation is actually observed in locations such as Florida. It is possible that the increase in atmospheric moisture in the HMG case also further smooths the temperature field and compounds decreasing MsKE. Decreasing sensible heat flux, and overall heating from the change in EF, is also likely a contributor to the changes (or lack thereof) in regions that are not moisture limited. Changes in energy from heat, however, cannot perfectly explain the phenomena either, as evidenced by the lack of change, or slight increase, in the temperature field over most of the domain.

Many of these phenomena can be understood as an interplay between the increasing moisture, EF, and decreasing boundary layer flow activity. For much of the domain, where no sustained increase in precipitation is observed (figure 6), the moisture supply is increased while the mesoscale motion that promotes convective initiation decreases. When averaged over the 257 simulation days, this results in no net precipitation increases. This does, however, result in a continuous decrease in the accuracy of precipitation events each day (figure 5c) as, in any given day, moisture availability, sensible heating, or convective initiation may be a more important factor in the spatiotemporal patterns of precipitation. There are locations where the increase in moisture availability is a deciding factor in precipitation events. These appear to be mostly locations with low average EF, including the northern Great Lakes (GRL) and gulf of California (MEX) (see figure 8a) where sustained increases in precipitation occur. In Florida and parts of the Gulf Coast and East Coast, however, EF is very high as is moisture availability. The deciding factor for spatiotemporal patterns of many precipitation events in these regions, therefore, may be whether sufficient flow from sea breeze events exists to promote movement of that moisture beyond the level of free convection to trigger convective precipitation. Change in $MsKE_{low}$ also likely plays a role, along with changes to sensible heating as more energy is partitioned into moisture flux, in the lack of changes in precipitation in other regions of the domain. The reduced energy from heating and from reduced mesoscale heterogeneity driven flows prevents the increased moisture from causing precipitation. Additionally, all of these factors are compounded by where the homogenization most changes the fluxes by decreasing variability (figure 3). Much of the Midwest (part of CTL), for example, has very low spatial variability in latent and sensible heat fluxes, and as a result there is little signature of change due to homogenization in EF, precipitation, or $MsKE_{low}$. The non-response, in the precipitation field at least, to homogenization in inland domains could also be a partial consequence of a feedback with precipitation. Studies show that, under breeze like circulations and secondary circulations, cloud formation and precipitation preferentially occurs over the drier, warmer area (Avissar and Liu 1996; Simon et al. 2021; Lee et al. 2019; Rochetin et al. 2017; Klein and Taylor 2020). This will, accordingly, result in a homogenization of the field as the drier area becomes wet. In some situations, this could even cause the flux field to be more homogeneous in the HET case than the HMG case. While the impacts of aphysical changes in moisture caused by homogenization are clear, more work needs to be done to understand the role of heterogeneity driven flows and mesoscale kinetic energy of the boundary layer, which are significantly reduced across the domain and have a clear impact in the Southeast, in land-atmosphere coupling.

b. Applications to Earth System Modelling and Coarse Resolution Weather Prediction

The results show that significant care should be taken when homogenizing a finer resolution surface (land and ocean) with a coarser resolution atmosphere, whether this occurs through an explicitly higher resolution grid or an effectively higher resolution grid via an LSM tiling scheme. Errors, biases, and changes in precipitation, cloud cover, temperature, and atmospheric moisture are especially concerning in highly variable regions. This is most significant when bodies of water (lakes, rivers and ocean) are homogenized with land tiles. In addition to the high gradients in these areas, bodies of water have no capacity to dry out, like a wet land homogenized with dry land could, promoting a continual release of moisture that is, by virtue of the homogenization, immediately transported from over open water over to dry land where it no longer works to suppress more evaporation from the open water. Surface-atmosphere coupling should ideally be designed in a way to avoid having water and land under the same atmospheric grid. If they are averaged together, active attempts need to be made to prevent overestimation of resulting evaporation.

Additionally, the role of mesoscale and sub-mesoscale boundary layer activity driven by heterogeneity needs to be properly parameterized. Biases in coastal temperatures as well as precipitation in energy limited regions with significant gradients (Florida) can occur if it is not properly considered. Results from this work and the literature suggest that significant changes in spatiotemporal patterns of precipitation and cloud development may occur on the daily scale, even if they don't occur on the seasonal scale, which is certainly relevant for NWP and could have other effects relevant for the climate modeling community. Additional investigation, however, is necessary to fully evaluate the impact on specific events and for shorter time scales. Any future parameterization of sub-grid heterogeneity-driven also needs to consider that models can only resolve heterogeneity-driven circulations when the heterogeneity is on the order of 4 times the grid scale (Zheng et al. 2021). Model parameterizations would also benefit from considering the explicit spatial organization of the sub-grid heterogeneity, which is often neglected in tiling schemes(Fisher and Koven 2020), as larger scale circulations are more likely to occur only with sustained spatial heterogeneity. Two column models have strong potential to represent structured mesoscale flows (Waterman et al. 2024), however they are computationally expensive. Integrating these ideas into multi-plume mass flux additions to boundary layer schemes (Sušelj et al. 2013; Witte et al. 2022) has potential for more computationally efficient representation, although such models have yet to be explored in detail or broadly applied.

c. Challenges and Considerations

There are a number of challenges and limitations of the study that are important to consider when evaluating the results. In both the HET and HMG case, there was a persistent observed energy balance residual around -2.5 Wm^{-2} in the HET case and -7 Wm^{-2} in the HMG case, which may influence the results. It is worth noting, however, that due to the 48 hour simulation length, the sea surface temperatures were set to non-updating, which means that ocean water heating is not accounted for in the energy balance and is likely where this ”missing energy” could go. As mentioned previously, models require heterogeneity scales on the order of 4 times the atmospheric grid scale to properly resolve many heterogeneity driven flows. As such, the simulations in this study do not properly consider smaller scale secondary circulations which will likely be relevant for land-atmosphere coupling, especially in finer resolution NWP schemes. Long term effects are also not considered as part of this study. The 48 hour simulation time scale is useful for more meaningful and direct comparison between the heterogeneous and homogeneous cases, but it admittedly does not account for long term effects, such as the ”memory” of the soil moisture to the precipitation events which can be very impactful for seasonal simulations (Knist et al. 2020).

In addition, the role of MsKE requires more thorough exploration. MsKE also captures background perturbations in addition to heterogeneity driven flows, and larger scale dynamics and convection. The background perturbations are likely low based on low observed baseline values of MsKE. Further examination of MsKE under weak synoptic scale forcing (i.e. clear sky, low background wind) conditions would both allow for analysis that removes the larger scale convective storm imprint on MsKE as well as highlight the days where heterogeneity driven flows are expected to have the greatest impact on the atmosphere. Initial work in this area is promising, however deeper analysis in a subsequent publication is necessary.

The study primarily focused on homogenization of the surface fluxes. It is worth noting, however, that two other forms of homogenization that occur in ESMs were not included here. Studies have shown that the smoothing of topography at the larger grid scales has significant impacts on sub-grid scale motion, precipitation, and cloud development (Knist et al. 2020; Zhao and Li 2015; Wagner et al. 2015). ESMs, due to the coarser atmospheric grid, often pass coarse resolution precipitation back to the land, whereas these simulations maintain the 3 km resolution precipitation. Previous work has shown that, in some places, rainfall and other meteorological characteristics can drive a significant portion of the surface heterogeneity (Simon et al. 2021; Guillod et al. 2015; Li et al. 2020). Studies also show precipitation can have high spatial bias, especially in heterogeneous land surface regimes (Avissar and Liu 1996; Simon et al. 2021; Lee et al. 2019).

5. Conclusion

In this study, we run 48 hour WRF simulations for every day in the summers (JJA) of 2021, 2022, and 2023 over CONUS at 3 km, with a default heterogeneous case (HET) and a homogeneous case (HMG) where the surface fluxes and skin temperature are homogenized to 60 km resolution at every time step. We separately examined how choosing different homogenization scales would affect one, 48 hour simulation period. The homogenization is analogous to the homogenization that occurs in ESMs when LSM tiling schemes or higher resolution land and ocean models have surface fluxes homogenized to an overlying atmosphere. Results, overall, show dramatic changes in cloud production and precipitation over the three summers due to homogenization driven by two often counteracting phenomena. The homogenization between wet and dry areas, particularly open water (lakes, rivers, ocean) and land, causes an increase in moisture fluxes from the wet area and a resulting increase in evaporative fraction EF. The changes to EF increase the moisture in the boundary layer significantly, promoting increased precipitation and cloud development. The homogenization also causes a reduction in the strength of mesoscale flows and convective plumes in the ABL, represented by $MsKE_{low}$, likely due to a dampening or elimination of flows driven by heterogeneity such as sea/lake breezes, and secondary circulations. The reduction of these flows causes a decrease in cloud development and precipitation. Overall, the increase in EF appears to be the dominant mechanism effecting precipitation changes broadly. This is especially true in dry moisture limited regions, such as the Gulf of California during the North American Monsoon season, and north of the Great Lakes, which experience a nearly 100% (200 mm+) and 50% (50-100 mm) increase respectively in mean cumulative summer precipitation in the HMG case when compared to the HET case. For most of the domain, the increase in moisture availability, clear in maps of low level clouds, RH_{2m}, and PW, does not translate to a strong increase in rainfall likely due to a slight decrease in sensible heating as well as a change in mesoscale flow activity in the boundary layer, $MsKE_{low}$. While decreasing sensible heating implied by the increased EF may be a primary reason, this is unlikely to explain it alone as the field of temperature appears largely unaffected or slightly increased by homogenization outside of coastal regions where increases are more significant and counter-intuitive to the changes in EF. Regions with high moisture availability, such as the Florida peninsula, however, experience decreases in precipitation with homogenization likely due to the reduced opportunities for convective initiation from dampened sea breezes. Results overall show that careful consideration of surface heterogeneity is necessary for coupling of the surface and atmosphere in ESMs and coarse grid NWP. This consideration is particularly important in regions where fluxes from open water are homogenized with fluxes over land, and where high spatial gradients are present in the flux fields.

Acknowledgments. This research has been supported by NA19OAR4310241 - Parameterizing the effects of sub-grid land heterogeneity on the atmospheric boundary layer and convection: Implications for surface climate, variability, and extremes. As well as NA220AR0AR4310644 - Implications of heterogeneity-aware land-atmosphere coupling in the predictability of precipitation extremes.

Data availability statement. Data used to conduct this research is entirely publically available.

HRRR data used to provide initial and boundary conditions can be accessed through a NOAA AWS server at https://registry.opendata.aws/noaa-hrrr-pds.

MSWEP precipitation data can be accessed via https://www.gloh2o.org/mswep/

Modified Weather Research and Forecasting Model (WRF) code, as well as the WRF namelists and scripts used to complete this work has been made publicly available (Waterman 2024).

References

Akinlabi, E., B. Maronga, M. G. Giometto, and D. Li, 2022: Dispersive Fluxes Within and Over a Real Urban Canopy: A Large-Eddy Simulation Study. *Boundary-Layer Meteorology*, **185 (1)**, 93–128, https://doi.org/10.1007/s10546-022-00725-6.

Avissar, R., and Y. Liu, 1996: Three-dimensional numerical study of shallow convective clouds and precipitation induced by land surface forcing. *Journal of Geophysical Research: Atmospheres*, **101 (D3)**, 7499–7518, https://doi.org/10.1029/95JD03031.

Barlage, M., F. Chen, R. Rasmussen, Z. Zhang, and G. Miguez-Macho, 2021: The Importance of Scale-Dependent Groundwater Processes in Land-Atmosphere Interactions Over the Central United States. *Geophysical Research Letters*, **48 (5)**, e2020GL092 171, https://doi.org/10.1029/2020GL092171.

Beck, H. E., E. F. Wood, M. Pan, C. K. Fisher, D. G. Miralles, A. I. J. M. Van Dijk, T. R. McVicar, and R. F. Adler, 2019: MSWEP V2 Global 3-Hourly 0.1° Precipitation: Methodology and Quantitative Assessment. *Bulletin of the American Meteorological Society*, **100 (3)**, 473–500, https://doi.org/10.1175/BAMS-D-17-0138.1.

Birch, C. E., M. J. Roberts, L. Garcia-Carreras, D. Ackerley, M. J. Reeder, A. P. Lock, and R. Schiemann, 2015: Sea-Breeze Dynamics and Convection Initiation: The Influence of Convective Parameterization in Weather and Climate Model Biases. *Journal of Climate*, **28 (20)**, 8093–8108, https://doi.org/10.1175/JCLI-D-14-00850.1.

Bonan, G. B., K. W. Oleson, M. Vertenstein, S. Levis, X. Zeng, Y. Dai, R. E. Dickinson, and Z.-L. Yang, 2002: The Land Surface Climatology of the Community Land Model Coupled to the NCAR Community Climate Model*. *Journal of Climate*, **15 (22)**, 3123–3149, https://doi.org/10.1175/1520-0442(2002)015⟨3123:TLSCOT⟩2.0.CO;2.

Bou-Zeid, E., W. Anderson, G. G. Katul, and L. Mahrt, 2020: The Persistent Challenge of Surface Heterogeneity in Boundary-Layer Meteorology: A Review. *Boundary-Layer Meteorology*, **177 (2-3)**, 227–245, https://doi.org/10.1007/s10546-020-00551-8.

Chaney, N. W., L. Torres-Rojas, N. Vergopolan, and C. K. Fisher, 2021: HydroBlocks v0.2: enabling a field-scale two-way coupling between the land surface and river networks in Earth system models. *Geoscientific Model Development*, **14 (11)**, 6813–6832, https://doi.org/10.5194/gmd-14-6813-2021.

Chaney, N. W., and Coauthors, 2019: POLARIS Soil Properties: 30-m Probabilistic Maps of Soil Properties Over the Contiguous United States. *Water Resources Research*, **55 (4)**, 2916–2938, https://doi.org/10.1029/2018WR022797.

Crosman, E. T., and J. D. Horel, 2010: Sea and Lake Breezes: A Review of Numerical Studies. *Boundary-Layer Meteorology*, **137 (1)**, 1–29, https://doi.org/10.1007/s10546-010-9517-9.

Danabasoglu, G., and Coauthors, 2020: The Community Earth System Model Version 2 (CESM2). *Journal of Advances in Modeling Earth Systems*, **12 (2)**, e2019MS001 916, https://doi.org/10.1029/2019MS001916.

De Vrese, P., and S. Hagemann, 2016: Explicit Representation of Spatial Subgrid-Scale Heterogeneity in an ESM. *Journal of Hydrometeorology*, **17 (5)**, 1357–1371, https://doi.org/10.1175/JHM-D-15-0080.1.

De Vrese, P., J.-P. Schulz, and S. Hagemann, 2016: On the Representation of Heterogeneity in Land-Surface–Atmosphere Coupling. *Boundary-Layer Meteorology*, **160 (1)**, 157–183, https://doi.org/10.1007/s10546-016-0133-1.

Dowell, D. C., and Coauthors, 2022: The High-Resolution Rapid Refresh (HRRR): An Hourly Updating Convection-Allowing Forecast Model. Part I: Motivation and System Description. *Weather and Forecasting*, **37 (8)**, 1371–1395, https://doi.org/10.1175/WAF-D-21-0151.1.

Ducharne, A., R. D. Koster, M. J. Suarez, M. Stieglitz, and P. Kumar, 2000: A catchment-based approach to modeling land surface processes in a general circulation model: 2. Parameter estimation and model demonstration. *Journal of Geophysical Research: Atmospheres*, **105 (D20)**, 24 823–24 838, https://doi.org/10.1029/2000JD900328.

Dunne, J. P., and Coauthors, 2020: The GFDL Earth System Model Version 4.1 (GFDL-ESM 4.1): Overall Coupled Model Description and Simulation Characteristics. *Journal of Advances in Modeling Earth Systems*, **12 (11)**, e2019MS002 015, https://doi.org/10.1029/2019MS002015.

Fisher, R. A., and C. D. Koven, 2020: Perspectives on the Future of Land Surface Models and the Challenges of Representing Complex Terrestrial Systems. *Journal of Advances in Modeling Earth Systems*, **12 (4)**, e2018MS001 453, https://doi.org/10.1029/2018MS001453.

Garcia-Carreras, L., D. J. Parker, and J. H. Marsham, 2011: What is the Mechanism for the Modification of Convective Cloud Distributions by Land Surface–Induced Flows? *Journal of the Atmospheric Sciences*, **68 (3)**, 619–634, https://doi.org/10.1175/2010JAS3604.1.

Golaz, J., and Coauthors, 2022: The DOE E3SM Model Version 2: Overview of the Physical Model and Initial Model Evaluation. *Journal of Advances in Modeling Earth Systems*, **14 (12)**, e2022MS003 156, https://doi.org/10.1029/2022MS003156.

Guillod, B. P., B. Orlowsky, D. G. Miralles, A. J. Teuling, and S. I. Seneviratne, 2015: Reconciling spatial and temporal soil moisture effects on afternoon rainfall. *Nature Communications*, **6 (1)**, 6443, https://doi.org/10.1038/ncomms7443.

Hadfield, M. G., W. R. Cotton, and R. A. Pielke, 1991: Large-eddy simulations of thermally forced circulations in the convective boundary layer. Part I: A small-scale circulation with zero wind. *Boundary-Layer Meteorology*, **57 (1-2)**, 79–114, https://doi.org/10.1007/BF00119714.

Han, C., S. Brdar, and S. Kollet, 2019: Response of Convective Boundary Layer and Shallow Cumulus to Soil Moisture Heterogeneity: A Large-Eddy Simulation Study. *Journal of Advances in Modeling Earth Systems*, **11 (12)**, 4305–4322, https://doi.org/10.1029/2019MS001772.

Held, I. M., and Coauthors, 2019: Structure and Performance of GFDL's CM4.0 Climate Model. *Journal of Advances in Modeling Earth Systems*, **11 (11)**, 3691–3727, https://doi.org/10.1029/2019MS001829.

Hock, N., F. Zhang, and Z. Pu, 2022: Numerical Simulations of a Florida Sea Breeze and Its Interactions with Associated Convection: Effects of Geophysical Representation and Model Resolution. *Advances in Atmospheric Sciences*, **39 (5)**, 697–713, https://doi.org/10.1007/s00376-021-1216-6.

Hohenegger, C., and C. Schar, 2007: Atmospheric Predictability at Synoptic Versus Cloud-Resolving Scales. *Bulletin of the American Meteorological Society*, **88 (11)**, 1783–1794, https://doi.org/10.1175/BAMS-88-11-1783.

Huang, M., P.-L. Ma, N. W. Chaney, D. Hao, G. Bisht, M. D. Fowler, V. E. Larson, and L. R. Leung, 2022: Representing surface heterogeneity in land–atmosphere coupling in E3SMv1 single-column model over ARM SGP during summertime. *Geoscientific Model Development*, **15 (16)**, 6371–6384, https://doi.org/10.5194/gmd-15-6371-2022.

Iacono, M. J., J. S. Delamere, E. J. Mlawer, M. W. Shephard, S. A. Clough, and W. D. Collins, 2008: Radiative forcing by long-lived greenhouse gases: Calculations with the AER radiative transfer models. *Journal of Geophysical Research: Atmospheres*, **113 (D13)**, 2008JD009 944, https://doi.org/10.1029/2008JD009944.

Iorio, J. P., P. B. Duffy, B. Govindasamy, S. L. Thompson, M. Khairoutdinov, and D. Randall, 2004: Effects of model resolution and subgrid-scale physics on the simulation of precipitation in the continental United States. *Climate Dynamics*, **23 (3-4)**, 243–258, https://doi.org/10.1007/s00382-004-0440-y.

Jung, M., and Coauthors, 2011: Global patterns of land-atmosphere fluxes of carbon dioxide, latent heat, and sensible heat derived from eddy covariance, satellite, and meteorological observations. *Journal of Geophysical Research*, **116**, G00J07, https://doi.org/10.1029/2010JG001566.

Klein, C., and C. M. Taylor, 2020: Dry soils can intensify mesoscale convective systems. *Proceedings of the National Academy of Sciences*, **117 (35)**, https://doi.org/10.1073/pnas.2007998117.

Knist, S., K. Goergen, and C. Simmer, 2020: Effects of land surface inhomogeneity on convection-permitting WRF simulations over central Europe. *Meteorology and Atmospheric Physics*, **132 (1)**, 53–69, https://doi.org/10.1007/s00703-019-00671-y.

Koch, J., G. Mendiguren, G. Mariethoz, and S. Stisen, 2017: Spatial Sensitivity Analysis of Simulated Land Surface Patterns in a Catchment Model Using a Set of Innovative Spatial Performance Metrics. *Journal of Hydrometeorology*, **18 (4)**, 1121–1142, https://doi.org/10.1175/JHM-D-16-0148.1.

Lee, J. M., Y. Zhang, and S. A. Klein, 2019: The Effect of Land Surface Heterogeneity and Background Wind on Shallow Cumulus Clouds and the Transition to Deeper Convection. *Journal of the Atmospheric Sciences*, **76 (2)**, 401–419, https://doi.org/10.1175/JAS-D-18-0196.1.

Li, J., T. Y. Gan, Y. D. Chen, X. Gu, Z. Hu, Q. Zhou, and Y. Lai, 2020: Tackling resolution mismatch of precipitation extremes from gridded GCMs and site-scale observations: Implication to assessment and future projection. *Atmospheric Research*, **239**, 104 908, https://doi.org/10.1016/j.atmosres.2020.104908.

Manrique-Suñén, A., A. Nordbo, G. Balsamo, A. Beljaars, and I. Mammarella, 2013: Representing Land Surface Heterogeneity: Offline Analysis of the Tiling Method. *Journal of Hydrometeorology*, **14 (3)**, 850–867, https://doi.org/10.1175/JHM-D-12-0108.1.

Miller, S. T. K., B. D. Keim, R. W. Talbot, and H. Mao, 2003: Sea breeze: Structure, forecasting, and impacts: SEA BREEZE. *Reviews of Geophysics*, **41 (3)**, https://doi.org/10.1029/2003RG000124.

Nakanishi, M., and H. Niino, 2009: Development of an Improved Turbulence Closure Model for the Atmospheric Boundary Layer. *Journal of the Meteorological Society of Japan. Ser. II*, **87 (5)**, 895–912, https://doi.org/10.2151/jmsj.87.895.

Naumann, A. K., B. Stevens, and C. Hohenegger, 2019: A Moist Conceptual Model for the Boundary Layer Structure and Radiatively Driven Shallow Circulations in the Trades. *Journal of the Atmospheric Sciences*, **76 (5)**, 1289–1306, https://doi.org/10.1175/JAS-D-18-0226.1.

Olson, J. B., J. S. Kenyon, W. A. Angevine, J. M. Brown, M. Pagowski, and K. Sušelj, 2019: A Description of the MYNN-EDMF Scheme and the Coupling to Other Components in WRF–ARW. https://doi.org/10.25923/N9WM-BE49.

Rochetin, N., F. Couvreux, and F. Guichard, 2017: Morphology of breeze circulations induced by surface flux heterogeneities and their impact on convection initiation: Breeze Circulations Induced by Surface Heterogeneities. *Quarterly Journal of the Royal Meteorological Society*, **143 (702)**, 463–478, https://doi.org/10.1002/qj.2935.

Santanello, J. A., and Coauthors, 2018: Land–Atmosphere Interactions: The LoCo Perspective. *Bulletin of the American Meteorological Society*, **99 (6)**, 1253–1272, https://doi.org/10.1175/BAMS-D-17-0001.1.

Satoh, M., B. Stevens, F. Judt, M. Khairoutdinov, S.-J. Lin, W. M. Putman, and P. Düben, 2019: Global Cloud-Resolving Models. *Current Climate Change Reports*, **5 (3)**, 172–184, https://doi.org/10.1007/s40641-019-00131-0.

Segal, M., and R. W. Arritt, 1992: Nonclassical Mesoscale Circulations Caused by Surface Sensible Heat-Flux Gradients. *Bulletin of the American Meteorological Society*, **73 (10)**, 1593–1604, https://doi.org/10.1175/1520-0477(1992)073⟨1593:NMCCBS⟩2.0.CO;2.

Simon, J. S., A. D. Bragg, P. A. Dirmeyer, and N. W. Chaney, 2021: Semi-Coupling of a Field-Scale Resolving Land-Surface Model and WRF-LES to Investigate the Influence of Land-Surface Heterogeneity on Cloud Development. *Journal of Advances in Modeling Earth Systems*, **13 (10)**, https://doi.org/10.1029/2021MS002602.

Skamarock, W. C., S.-H. Park, J. B. Klemp, and C. Snyder, 2014: Atmospheric Kinetic Energy Spectra from Global High-Resolution Nonhydrostatic Simulations. *Journal of the Atmospheric Sciences*, **71 (11)**, 4369–4381, https://doi.org/10.1175/JAS-D-14-0114.1.

Skamarock, W. C., and Coauthors, 2021: A Description of the Advanced Research WRF Model Version 4. https://doi.org/10.5065/1dfh-6p97.

Smirnova, T. G., J. M. Brown, S. G. Benjamin, and J. S. Kenyon, 2016: Modifications to the Rapid Update Cycle Land Surface Model (RUC LSM) Available in the Weather Research and Forecasting (WRF) Model. *Monthly Weather Review*, **144 (5)**, 1851–1865, https://doi.org/10.1175/MWR-D-15-0198.1.

Šušelj, K., J. Teixeira, and D. Chung, 2013: A Unified Model for Moist Convective Boundary Layers Based on a Stochastic Eddy-Diffusivity/Mass-Flux Parameterization. *Journal of the Atmospheric Sciences*, **70 (7)**, 1929–1953, https://doi.org/10.1175/JAS-D-12-0106.1.

Thompson, G., and T. Eidhammer, 2014: A Study of Aerosol Impacts on Clouds and Precipitation Development in a Large Winter Cyclone. *Journal of the Atmospheric Sciences*, **71 (10)**, 3636–3658, https://doi.org/10.1175/JAS-D-13-0305.1.

Toll, D. L., J. K. Entin, and P. R. Houser, 2002: Land surface heterogeneity on surface energy and water fluxes. *Proceedings of SPIE*, M. Owe, and G. D'Urso, Eds., Toulouse, France, 267, https://doi.org/10.1117/12.454209, URL http://proceedings.spiedigitallibrary.org/proceeding.aspx?doi=10.1117/12.454209.

Torres-Rojas, L., N. Vergopolan, J. D. Herman, and N. W. Chaney, 2022: Towards an Optimal Representation of Sub-Grid Heterogeneity in Land Surface Models. *Water Resources Research*, **58 (12)**, https://doi.org/10.1029/2022WR032233.

van Heerwaarden, C. C., J. P. Mellado, and A. De Lozar, 2014: Scaling Laws for the Heterogeneously Heated Free Convective Boundary Layer. *Journal of the Atmospheric Sciences*, **71 (11)**, 3975–4000, https://doi.org/10.1175/JAS-D-13-0383.1.

Vergopolan, N., and Coauthors, 2022: High-Resolution Soil Moisture Data Reveal Complex Multi-Scale Spatial Variability Across the United States. *Geophysical Research Letters*, **49 (15)**, e2022GL098 586, https://doi.org/10.1029/2022GL098586.

Wagner, J. S., A. Gohm, and M. W. Rotach, 2015: The impact of valley geometry on daytime thermally driven flows and vertical transport processes. *Quarterly Journal of the Royal Meteorological Society*, **141 (690)**, 1780–1794, https://doi.org/10.1002/qj.2481.

Waterman, T., 2024: Data for: Semi-coupling of a Field-scale Resolving Land-surface Model and WRF-LES to Investigate the Influence of Land-surface Heterogeneity on Cloud Development. Zenodo, URL https://zenodo.org/doi/10.5281/zenodo.12556465, https://doi.org/10.5281/zenodo.12556466.

Waterman, T., A. D. Bragg, F. Hay-Chapman, P. A. Dirmeyer, M. D. Fowler, J. Simon, and N. Chaney, 2024: A Two-Column Model Parameterization for Subgrid Surface Heterogeneity

Driven Circulations. *Journal of Advances in Modeling Earth Systems*, **16 (5)**, e2023MS003 936, https://doi.org/10.1029/2023MS003936.

Weaver, C. P., 2004: Coupling between Large-Scale Atmospheric Processes and Mesoscale Land–Atmosphere Interactions in the U.S. Southern Great Plains during Summer. Part I: Case Studies. *Journal of Hydrometeorology*, **5 (6)**, 1223–1246, https://doi.org/10.1175/JHM-396.1.

Weaver, C. P., S. Baidya Roy, and R. Avissar, 2002: Sensitivity of simulated mesoscale atmospheric circulations resulting from landscape heterogeneity to aspects of model configuration. *Journal of Geophysical Research: Atmospheres*, **107 (D20)**, https://doi.org/10.1029/2001JD000376.

Witte, M. K., and Coauthors, 2022: Augmenting the Double-Gaussian Representation of Atmospheric Turbulence and Convection via a Coupled Stochastic Multi-Plume Mass-Flux Scheme. *Monthly Weather Review*, **150 (9)**, 2339–2355, https://doi.org/10.1175/MWR-D-21-0215.1.

Xu, C., L. Torres-Rojas, N. Vergopolan, and N. W. Chaney, 2023: The Benefits of Using State-Of-The-Art Digital Soil Properties Maps to Improve the Modeling of Soil Moisture in Land Surface Models. *Water Resources Research*, **59 (4)**, e2022WR032 336, https://doi.org/10.1029/2022WR032336.

Zhang, L., S. Poll, and S. Kollet, 2023: Large-eddy simulation of soil moisture heterogeneity-induced secondary circulation with ambient winds. *Quarterly Journal of the Royal Meteorological Society*, **149 (751)**, 404–420, https://doi.org/10.1002/qj.4413.

Zhang, N., Q. L. Williams, and H. Liu, 2010: Effects of land-surface heterogeneity on numerical simulations of mesoscale atmospheric boundary layer processes. *Theoretical and Applied Climatology*, **102 (3-4)**, 307–317, https://doi.org/10.1007/s00704-010-0268-9.

Zhao, W., and A. Li, 2015: A Review on Land Surface Processes Modelling over Complex Terrain. *Advances in Meteorology*, **2015**, 1–17, https://doi.org/10.1155/2015/607181.

Zheng, Y., N. A. Brunsell, J. G. Alfieri, and D. Niyogi, 2021: Impacts of land cover heterogeneity and land surface parameterizations on turbulent characteristics and mesoscale simulations. *Meteorology and Atmospheric Physics*, **133 (3)**, 589–610, https://doi.org/10.1007/s00703-020-00768-9.